# Comparison of theory and direct numerical simulations of drag reduction by rodlike polymers in turbulent channel flows

Roberto Benzi,[1] Emily S. C. Ching,[2] Elisabetta De Angelis,[3] and Itamar Procaccia[4]

[1]*Dipartimento di Fisica and INFN, Università di Roma "Tor Vergata", Via della Ricerca Scientifica 1, 00133 Roma, Italy*
[2]*Department of Physics and Institute of Theoretical Physics, The Chinese University of Hong Kong, Shatin, Hong Kong*
[3]*II Facoltà di Ingegneria, Universit di Bologna, I-47100 Forlì, Italy*
[4]*Department of Chemical Physics, The Weizmann Institute of Science, Rehovot 76100, Israel*

Numerical simulations of turbulent channel flows, with or without additives, are limited in the extent of the Reynolds number (Re) and Deborah number (De). The comparison of such simulations to theories of drag reduction, which are usually derived for asymptotically high Re and De, calls for some care. In this paper we present a study of drag reduction by rodlike polymers in a turbulent channel flow using direct numerical simulation and illustrate how these numerical results should be related to the recently developed theory.

PACS number(s): 47.27.Rc

## I. INTRODUCTION

Drag reduction in wall-bounded turbulent flows can be achieved with the addition of either flexible or rodlike polymers [1,2]. The theory of drag reduction by either type of polymers is by now well established [3]. The theory for flexible polymers is supported by both experiments and numerical simulations while that for rodlike polymers has been compared mainly with laboratory experiments. More scant are numerical simulations of drag reduction by rodlike polymers, and some results became available only quite recently [4]. Comparisons of theory and simulations in this case must be done with care, since the available theory assumes high enough Reynolds number (Re) and Deborah number (De), in contrast to the situation in simulations where these crucial characteristic numbers are relatively low. To clarify the relation between the theory and the available numerical simulations, we present in this paper a comparison between numerical simulations and theoretical predictions adapted to the limited values of Re and De.

The equations of motion used for the numerical simulations are

$$\frac{\partial U_i}{\partial t} + U_j \frac{\partial}{\partial x_j} U_i = -\frac{\partial p}{\partial x_i} + \nu_0 \frac{\partial^2 U_i}{\partial x_j \, \partial x_j} + \frac{\partial \sigma_{ij}}{\partial x_j}, \quad (1)$$

supplemented by the incompressibility constraint $\partial U_i / \partial x_i = 0$ where $U$ is the velocity field, $p$ is the pressure, the units are chosen such that the fluid density is unity, $\nu_0$ is the kinematic viscosity of the neat fluid, and $\sigma_{ij}$ is the additional stress tensor due to the rodlike polymers.

The rodlike polymers are represented by rigid and neutrally buoyant elongated particles. The particles are assumed to be massless and have no inertia. The orientation of each polymer is given by a unit vector $\boldsymbol{n}$. In turbulent flows with strong shear such that thermal Brownian rotations can be neglected, the evolution equation for the second moment of the conformation tensor $\mathcal{R}_{ij} = \langle n_i n_j \rangle$ is given by [5]

$$\frac{\partial \mathcal{R}_{ij}}{\partial t} + U_k \frac{\partial \mathcal{R}_{ij}}{\partial x_k} = \mathcal{S}_{ik} \mathcal{R}_{kj} + \mathcal{S}_{jk} \mathcal{R}_{ki} - 2 \mathcal{S}_{kl} \mathcal{R}_{ijkl}, \quad (2)$$

where $\mathcal{R}_{ijkl} = \langle n_i n_j n_k n_l \rangle$ and $\mathcal{S}_{ij} = \partial U_i / \partial x_j$ is the velocity gradient. Moreover, in this non-Brownian limit, the tensor $\sigma_{ij}$ in Eq. (1) is given by [5,6]

$$\sigma_{ij} = 6 \nu_p S_{kl} \mathcal{R}_{ijkl}, \quad (3)$$

where $\nu_p$ is the polymeric contribution to the viscosity at vanishingly small and time-independent shear, and is proportional to the product of $\nu_0 \phi$ where $\phi$ is the volume fraction of the polymers. In [5] it was argued that these equations can be closed by the simple closure $\mathcal{R}_{ijkl} = \mathcal{R}_{ij} \mathcal{R}_{kl}$. Whether or not this simple closure is generally correct, our numerical simulations which are discussed below show that these equations of motion exhibit the phenomenon of drag reduction, and our task is to compare the numerical findings to the theory of drag reduction which is based on these equations.

## II. SIMULATIONS

The equations of motion are numerically integrated for a channel flow. The dimensions of the integration domain are $2\pi L \times 2L \times 1.2\pi L$ in the $x$ (streamwise), $y$ (wall-normal), and $z$ (spanwise) directions, respectively, with $L$ being the channel half width. The numerical formulation is a standard pseudospectral method with Fourier expansion in directions parallel to the wall and Chebyshev in the direction normal to the wall. The grid used is $128 \times 193 \times 64$. The direct numerical simulations (DNSs) were performed at a nominal Re $\equiv U_0 L / \nu_0$ of 10 000 for both the Newtonian flow (with $\eta_p \equiv 6\nu_p / \nu_0 = 0$) and for turbulent flow with rodlike polymers with $\eta_p = 25$, where $U_0$ is the mean velocity at the center of the channel. Both flows were forced on average with the same pressure drop $p' \equiv -\partial p / \partial x$, so the resulting Reynolds number based on the friction velocity is the same and equal to Re$_\tau \equiv \sqrt{p' L} L / \nu_0 = 300$. In channel geometry the only nonvanishing mean velocity component is $V(y) \equiv \langle U_x \rangle$. Accordingly we separate the velocity field into its mean and fluctuation, $\boldsymbol{U} = V\hat{x} + \boldsymbol{u}$. Below we use the wall units: $y^+ \equiv y \text{Re}_\tau / L$ and $V^+(y^+) \equiv V / \sqrt{p' L}$.
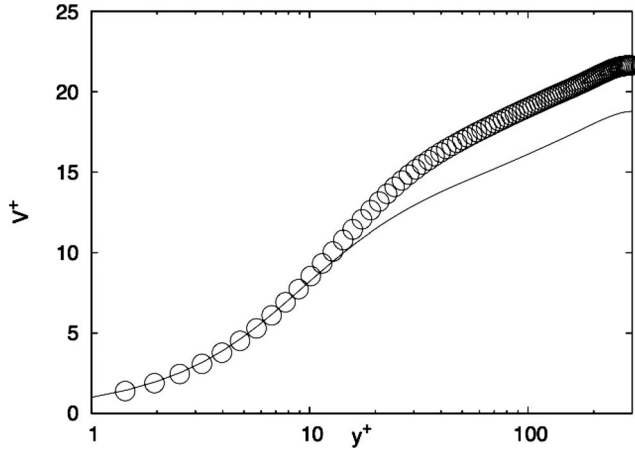
FIG. 1. Mean streamwise velocity profile $V^+(y^+)$ for both the Newtonian flow (solid line) and the rodlike polymer laden flow (circles). The amount of drag reduction obtained here is about 20%.

In the polymer laden flow, the mean velocity profile as a function of the distance from the wall (in wall units) exhibits an increase with respect to the Newtonian flow (see Fig. 1). This is the phenomenon of drag reduction. Note that the relative smallness of Re means here that the effect is not large, and by $y^+=80$ the velocity profile of the polymer laden flow is already parallel to that of the Newtonian flow. So any comparison with the theory of drag reduction should be limited to the rather narrow window of $20 < y^+ < 80$. One should note the very different situations here and when Re and De are very large. In the latter case, the mean velocity profile attains the maximum drag reduction asymptote (MDR) and never becomes parallel again to the von Kármán log law of the Newtonian flows.

In Fig. 2, we show the momentum fluxes. There is a significant reduction in the Reynolds stress $W(y) \equiv -\langle u_x u_y \rangle$ for the rodlike polymer laden flow as compared to the Newtonian flow. The Reynolds stress is the mean mechanical momentum flux from the fluid to the wall. It had been explained before that the reduction in the momentum flux is at the heart of the mechanism for drag reduction [7]. Let us note that Figs. 1 and 2 are quite close to what one observes in turbu-
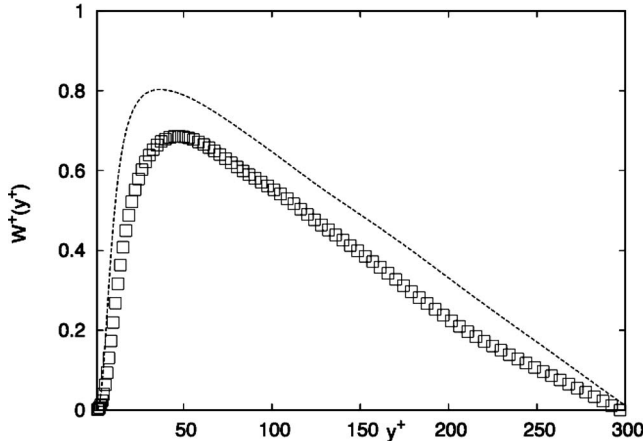


FIG. 2. The Reynolds stress $W(y)$ for the Newtonian flow (dashed line) and the flow with rodlike polymers (squares).

lent channel flows with flexible polymers: an increase of the mean velocity profile and a marked decrease of the mean momentum fluxes.

## III. COMPARISON OF THEORY WITH SIMULATIONS

The theory of turbulent drag reduction by rodlike polymers [6] is based in part on the exact momentum balance equation

$$\langle \sigma_{xy} \rangle + \nu_0 S + W = p'(L - y), \qquad (4)$$

where $S(y) = dV(y)/dy$ is the mean shear. A central ingredient of the theory is the statement (c.f. Eq. (44) in Ref. [6]) that the polymer contribution to this equation, i.e., $\langle \sigma_{xy} \rangle$, can be evaluated as

$$\langle \sigma_{xy} \rangle \approx c_1 \nu_p R_{yy}(y) S(y) \qquad (5)$$

with some constant $c_1$ and $R_{ij} = \langle \mathcal{R}_{ij} \rangle$. The intuitive reason for this evaluation can be understood directly from Eq. (3) in which $\langle S_{kl} \rangle = S \delta_{kx} \delta_{ly}$ forces one conformation tensor to be $R_{xy}$. Then a major contribution to the object $\langle \sigma_{xy} \rangle$ comes from a term in which the other conformation tensor is also $R_{xy}$. Since for a rigid polymer $R_{xx}$ is of order of unity, $R_{xy}^2$ is estimated as $R_{yy}$, leading to Eq. (5). Similarly, in the energy balance equation [6],

$$\nu_0 \langle s_{ij} s_{ij} \rangle + \langle \sigma_{ij} s_{ij} \rangle \approx SW, \qquad (6)$$

the polymer contribution to the dissipation, denoted here as $\epsilon^p = \langle \sigma_{ij} s_{ij} \rangle$, can be evaluated as

$$\epsilon^p(y) \approx c_2 \nu_p R_{yy}(y) \frac{K(y)}{y^2} \qquad (7)$$

with some constant $c_2$, where $K(y) \equiv \langle |u|^2 \rangle / 2$ is the kinetic energy of the fluctuating velocity. Here $s_{ij}$ is the fluctuating part of the velocity gradient tensor $\mathcal{S}_{ab}$, defined by

$$\mathcal{S}_{ab}(\mathbf{r}, t) = S(y) \delta_{ax} \delta_{by} + s_{ab}(\mathbf{r}, t), \quad \langle s_{ab}(\mathbf{r}, t) \rangle = 0. \qquad (8)$$

The spatial energy flux, which is known to be small in the log-law region, is neglected in Eq. (6).

The consequence of these results is the prediction that the effect of the polymers can be summarized by an additional effective viscosity, denoted below as the polymeric viscosity, proportional to $\nu_p R_{yy}(y)$. It was shown theoretically that for large Re and De these equations predict the establishment of a new velocity profile, again in the form a log law, but with a considerably larger slope compared to the Newtonian slope. This asymptotic log law is known as the maximum drag reduction asymptote (MDR). Moreover, the existence of a new log law, with $V^+$ linear in $\ln y^+$, for the (drag reduced) mean energy profile is directly related to $R_{yy}(y)$ increasing linearly with $y$. Physically, the theory states that the effects of the polymer can be treated as a $y$-dependent effective viscosity which increases linearly with $y$. It is thus of immediate interest to test these predictions also in the present case of relatively low Re and De. To this end, we show in Fig. 3 the averages of various components of the conformation tensors $R_{xx}$, $R_{yy}$, and $R_{xy}$ obtained in the simulation. We see clearly that $R_{yy}$ increases linearly with $y$ up to $y^+ \sim 80$, which
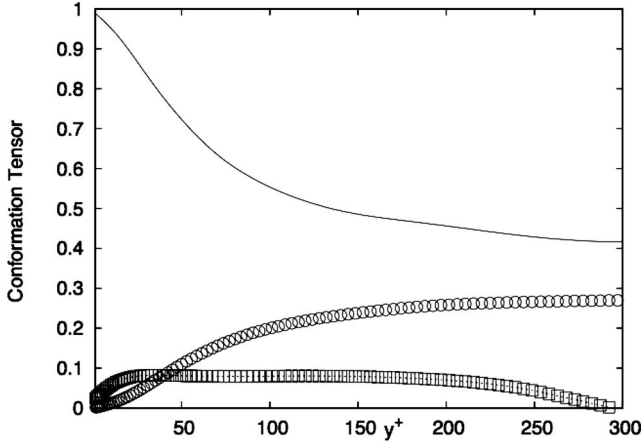
FIG. 3. The profiles of the averages of the components of the conformation tensor $R_{xx}$ (solid line), $R_{yy}$ (circles), and $R_{xy}$ (squares). $R_{zz}$ is not shown and is of the order of $R_{yy}$.

is the relevant range where drag reduction takes place in this simulation. In Fig. 4, we present the direct comparison of $\langle \sigma_{xy} \rangle$ with $\nu_p R_{yy}(y)S(y)$. The good agreement between the object and its evaluation is shown to exceed the region of linearity in $y^+$. Thus two central predictions of the theory are well supported by the direct numerical simulation even at the modest value of Re that is available here.

Needless to say, not every prediction of a theory that is developed as an *asymptotic* theory in the limit of Re $\rightarrow \infty$ and Deborah number De $\rightarrow \infty$ [6] can be expected to hold verbatim, and some modification might be required. In the asymptotic theory one argues that $R_{xx} \approx 1 \gg R_{xy}$, $R_{xy} \gg R_{yy}$, and $R_{yy} \sim R_{xy}^2$. We see from Fig. 3 that this is not the case here. To understand these results, note first that the Deborah number for flows with rodlike polymers is defined in the literature as De $\equiv S/\gamma_B$, where $\gamma_B$ is the Brownian rotational frequency. The simulations were done using $\gamma_B = 0$, formally at infinite De for a laminar shear flow. In the present case of a turbulent channel flow, the effect of turbulence is to induce
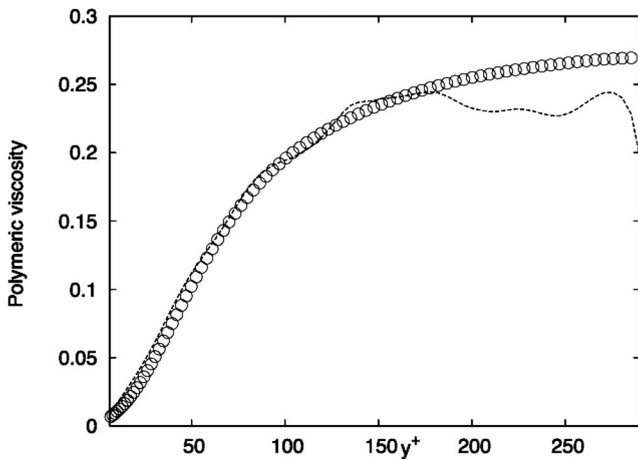


FIG. 4. A comparison of the polymeric viscosity in units of $\nu_p$, i.e., $R_{yy}(y^+)$ (dashed line) with $\langle \sigma_{xy} \rangle / c_1 \nu_p S(y^+)$ (circles). Note that $R_{yy}(y^+)$ is growing approximately linearly with $y^+$ as long as drag reduction exists (i.e., for $y^+ < 80$).

rotations of the polymers, giving rise to an effective relaxation frequency $\gamma_{turb}$ which depends on the turbulent intensity. Thus the corresponding effective Deborah number De $= S/\gamma_{turb}$ is also finite. At finite Re and finite De, the relative sizes of the averages of the various components of the conformation tensors need to be reevaluated. In the following, we shall show how the theory can be employed for the case of finite Re and De to explain the observed numerical results in Fig. 3.

We shall start from the equations of motions of the conformation tensor $\mathcal{R}_{ab}$. Averaging Eq. (2) over the turbulent fluctuations,

$$\left\langle U_k \frac{\partial \mathcal{R}_{ab}}{\partial x_k} \right\rangle = SR_{yb}\delta_{ax} + SR_{ya}\delta_{bx} + 2\delta_{ab}\frac{\Sigma}{3} - 2R_{ab}(R_{xy}S + \Sigma),$$

(9)

where $\Sigma = \langle \mathcal{R}_{ab}s_{ab} \rangle$. To derive this equation we first employed the closure assumption

$$\langle \mathcal{R}_{abcd}\mathcal{S}_{cd} \rangle \approx \langle \mathcal{R}_{ab}\mathcal{R}_{cd}\mathcal{S}_{cd} \rangle \approx R_{ab}(R_{xy}S + \Sigma). \quad (10)$$

The second simplification is the assumption that after removing the mean shear, the correlations of $s_{ab}$ and $\mathcal{R}_{ab}$ are not too far from isotropic, and in the log layer can also be taken as homogeneous. This implies:

$$\langle s_{xc}\mathcal{R}_{cx} \rangle \approx \langle s_{yc}\mathcal{R}_{cy} \rangle \approx \langle s_{zc}\mathcal{R}_{cz} \rangle \approx \frac{\Sigma}{3}, \quad (11)$$

$$\langle s_{ac}\mathcal{R}_{cb} \rangle \approx \delta_{ab}\frac{\Sigma}{3}. \quad (12)$$

Within the same assumptions we can also offer an approximate evaluation of $\Sigma \approx A\sqrt{W/y^2}$ since all the velocity fluctuations are close to isotropic. Here $A$ is a constant of the order of unity. Finally, we evaluate $\langle U_k \partial \mathcal{R}_{ab}/\partial x_k \rangle \approx 0$. This is seen by integrating by parts, using the incompressibility constraint, and neglecting the spatial flux of $\mathcal{R}_{ab}$ (which is consistent with neglecting the spatial energy flux). The derivative of the average is negligible for fluctuations that are not too far from homogeneous. With all these we obtain

$$0 = 2SR_{xy} - 2SR_{xx}R_{xy} - 2\Sigma\left(R_{xx} - \frac{1}{3}\right), \quad (13)$$

$$0 = SR_{yy} - 2R_{xy}^2 S - 2\Sigma R_{xy}, \quad (14)$$

$$0 = -2SR_{yy}R_{xy} - 2\Sigma\left(R_{yy} - \frac{1}{3}\right). \quad (15)$$

These equations are identical to those obeyed by the conformation tensor in a steady laminar shear flow and this tells us that $S/\Sigma$ can be taken as the effective $y$-*dependent* Deborah number in the simulation. Using Eqs. (13)–(15), we proceed to compute the $y$ profiles of $R_{ab}$. To do so, we solve $R_{ab}$ in terms of $S/\Sigma$. Taking into account that the situation we study is far from the MDR, we consider the effect of the polymers to be small perturbations and use the momentum and energy balance equations for turbulent Newtonian channel flow to
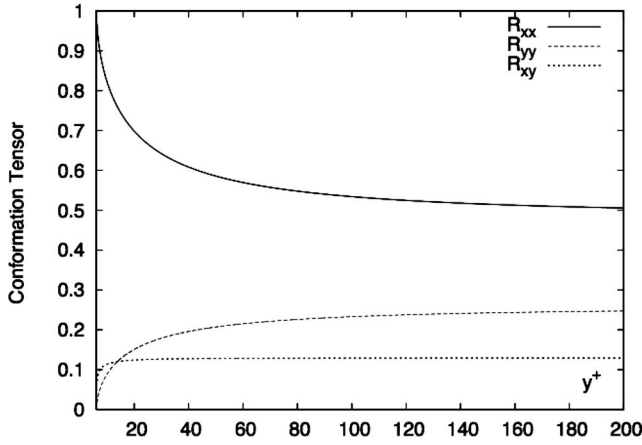
FIG. 5. Theoretical prediction of the averages of the components of the conformation tensor as a function of the distance from the wall.

get $S(y)$ and $W(y)$. Written in wall units, the momentum and energy balance equations for turbulent Newtonian channel flow read

$$S^+ + W^+ = 1 - \frac{y^+}{Re_\tau}, \qquad (16)$$

$$\frac{\delta^2}{y^{+2}} + \frac{\sqrt{W}}{\kappa_k y^+} = S^+, \qquad (17)$$

where $S^+ = S\nu_0/(p'L)$, $W^+ = W/(p'L)$, $\kappa_k$ is the von Kármán constant and $\delta$ is the thickness of the viscous layer in wall units which was found to be about 6 in [8].

In Fig. 5, we show $R_{xx}$, $R_{xy}$, and $R_{yy}$ obtained by solving Eqs. (13)–(15) with $A=0.7$. We find general agreement with the results shown in Fig. 3, explaining why in this case the relative sizes of the averages of the components of the conformation tensor differ from the predictions of the asymptotic theory. Our simple modeling can also explain the results shown in Fig. 4. We obtain from Eq. (14)

$$SR_{yy} = 2R_{xy}(SR_{xy} + \Sigma). \qquad (18)$$

Using this result and Eqs. (3) and (10), we get

$$\langle \sigma_{xy} \rangle \approx 6\nu_p R_{xy}(R_{xy}S + \Sigma) = 6\nu_p R_{yy}S. \qquad (19)$$

Thus even if the asymptotic theory cannot be applied directly in the present DNS, the basic prediction $\sigma_{xy} \approx c_1 \nu_p R_{yy} S$ still holds, consistent with the above mentioned approximations, i.e., neglecting anisotropic contributions like $\langle R_{xa}s_{ay} \rangle$.

In order to state that $R_{yy}$ is an effective viscosity it should also play the role of additional viscosity in the energy balance equation. To test the validity of this we compare the energy dissipation due to polymers $\epsilon^p$ against the theoretical prediction Eq. (7). This is done in Fig. 6. On the one hand, the results shown in Fig. 6 support our general conclusion that $\epsilon^p \sim R_{yy}K/y^2$ within a prefactor that we cannot estimate from the theory. On the other hand, the agreement is still not perfect; the measured $\epsilon^p$ shows two maxima as a function of $y^+$. The first peak is related to the maximum of $R_{yy}K/y^2$ while the second peak corresponds to the maximum of
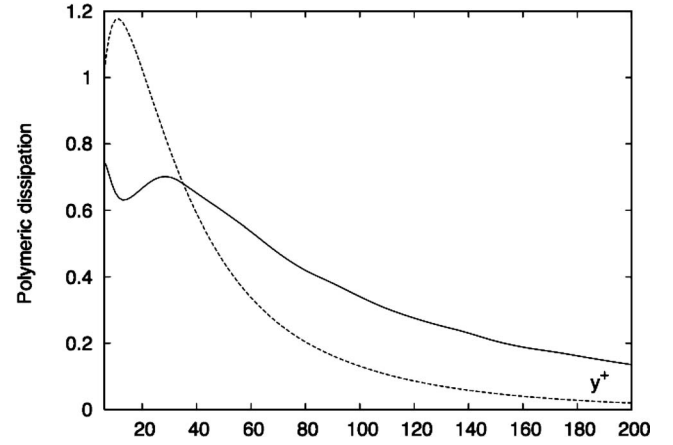


FIG. 6. Measured (solid line) and predicted (dotted line) dissipation contributed by the rodlike polymers to the energy balance equation. The measured quantity $\epsilon^p$ has two peaks, whereas $R_{yy}K/y^2$ has only one peak.

$\langle R_{xx}^2 s_{xx}^2 \rangle$. One of the central statements of the asymptotic theory [6] is that this term drops, by exact cancellation with another term, when the MDR is approached in De→∞. This is not occurring yet in our simulations with low Re and De.

From our numerical simulations and the theoretical analysis we can also state that $R_{yy}$ is linearly growing up to $y^+ \sim 80$. To see this, estimate the effect of linear viscosity profile using the following equations, which were derived and explained in great detail in [8]:

$$[1 + \alpha(y^+ - \delta)]S^+ + W^+ = 1, \qquad (20)$$

$$[1 + \alpha F(y^+ - \delta)]\frac{\Delta^2(\alpha)}{y^{+2}} + \frac{\sqrt{W^+}}{\kappa_k y^+} = S^+. \qquad (21)$$

In asymptotic conditions $F=1$, but here the factor $F$ takes into account that the effective slope of the linear viscosity
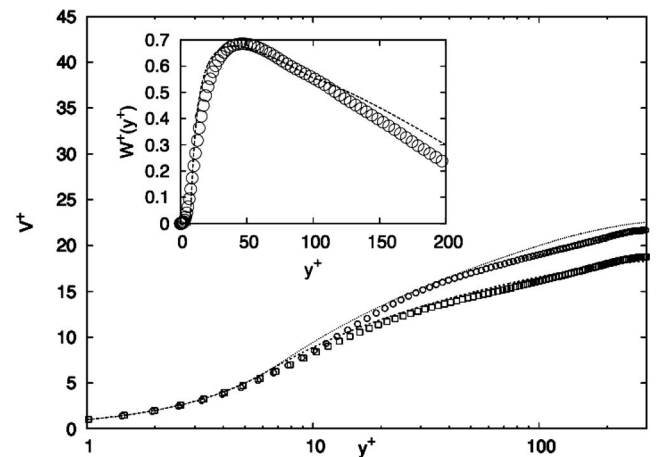


FIG. 7. Comparison of numerically computed profiles of $V^+(y^+)$ (circles) and $W^+(y^+)$ (circles in inset) with the results obtained from the balance equations [Eqs. (20) and (21)] (lines). We show also the comparison of $V^+(y^+)$ for flows without polymers (squares) with the results from Eqs. (20) and (21) using $\alpha=0$ (dashed line). The agreement is excellent.

profile is somehow smaller for the energy balance equation than for the momentum equation. According to our previous discussion on Fig. 6, we can estimate $F \approx 2$. In Eq. (21) the term $\Delta(\alpha)$ was determined theoretically [8]:

$$\Delta(\alpha) = \frac{\delta}{1 - \alpha\delta}. \qquad (22)$$

In our case the value of $\alpha$ is given by the relation

$$\alpha = \frac{\nu_p}{\nu} \frac{dR_{yy}}{dy}, \qquad (23)$$

where the slope $dR_{yy}/dy$ is estimated from the numerical simulation. Solving these simple coupled equations we present in Fig. 7 the quantities $V^+(y^+)$ and $W^+(y^+)$, respectively, for the Newtonian flow and for the polymer laden flow. Both figures agree well with the DNS.

## IV. CONCLUSIONS

The general philosophy behind our approach to drag reduction by additives is to consider the balance equations for mechanical momentum and turbulent energy, and to analyze the predictions of these equations for the profiles of the relevant quantities, in particular, the mean velocity at distance $y$ from the wall [3]. The theory can be simplified in the asymptotic regime when Re and De are very large; there one finds universal profiles, in particular, for the mean velocity profile which becomes the universal MDR [8]. For comparison with numerical simulations, where the drag reduction effect is rather limited due to small finite Re and De, one needs to analyze the balance equations with greater care, taking into account the nonasymptotic effects. This is what we have done in the present work, and our results are shown to agree well with the data obtained from direct numerical simulations.

[1] P. S. Virk, AIChE J. **21**, 615 (1975); P. S. Virk, D.C. Sherma, and D. L. Wagger, AIChE J. **43**, 3257 (1997).

[2] C. Wagner, Y. Amarouchène, P. Doyle, and D. Bonn, Europhys. Lett. **64**, 823 (2003).

[3] I. Procaccia, V.S. L'vov, and R. Benzi, Rev. Mod. Phys. **80**, 225 (2008).

[4] J. S. Paschkewitz, Y. Dubief, C. D. Dimitropoulos, E. S. G. Shaqfeh, and P. Moin, J. Fluid Mech. **518**, 281 (2004).

[5] M. Doi and S. F. Edwards, *The Theory of Polymer Dynamics* (Oxford, New York, 1988).

[6] R. Benzi, E. S. C. Ching, T. S. Lo, V.S. L'vov, and I. Procaccia, Phys. Rev. E **72**, 016305 (2005).

[7] V. S. L'vov, A. Pomyalov, I. Procaccia, and V. Tiberkevich, Phys. Rev. Lett. **92**, 244503 (2004).

[8] R. Benzi, E. De Angelis, V.S. L'vov, an I. Procaccia, Phys. Rev. Lett. **95**, 194502 (2005).